

Fast Proper Orthogonal Decomposition Using Improved Sampling and Iterative Techniques for Singular Value Decomposition

V. Charumathi¹, M. Ramakrishna¹, and Vinita Vasudevan¹

¹Indian Institute of Technology, Madras

Abstract

Proper Orthogonal Decomposition (POD), also known as Principal component analysis (PCA), is a well known dimensionality reduction technique that is used to capture the energetically dominant features of datasets, known as eigenfeatures or POD modes. The datasets involved are typically large, but correlated and have a relatively small number of dominant POD modes. These modes can be obtained by finding a low rank approximation of the data matrix using singular value decomposition (SVD). Since SVD computation is superlinear in the size of the matrix, both memory requirements and runtime are often prohibitive. Randomized algorithms have been proposed to obtain an approximate low rank description of the dataset in a computationally efficient manner. In this paper, we explore random sampling based techniques for approximate SVD computation. We first analyse the performance of two algorithms proposed by [1], namely LTSVD and CTSVD, and discuss their advantages and limitations. We modify the two algorithms to improve the runtime of the methods and prove the equivalence of our modified algorithms with LTSVD and CTSVD. The modifications we propose are independent of the sampling probability distribution and can be used to improve runtime whenever sampling is done with replacement. For large datasets, where memory is a bottleneck and the data has to be partitioned, we propose an algorithm that uses our modified algorithms in conjunction with a merging algorithm to compute the approximate SVD of the full matrix using the approximate SVDs of the partitions. We also propose an iterative algorithm to improve the approximation of the POD modes and the subspace spanned by the modes. Unlike the previous methods for multiple rounds of sampling, we obtain an updated approximation to the POD modes in each iteration and stop when the modes or subspace spanned by the modes have converged. The performance of our proposed solutions is analysed using four datasets of various sizes for single and multi-threaded execution. In all cases, we obtain a significant speedup over using a truncated SVD. The speedup of our modified LTSVD and CTSVD algorithms with respect to the existing algorithms depends on the error parameters and for low values of error parameters, we get upto $2-3\times$ speedup for the same accuracy. The results of the iterative algorithms have significantly better accuracies.

1 Introduction

Proper orthogonal decomposition (POD), also known as Principal component analysis (PCA) or Karhunen-Loeve transform is a dimensionality reduction technique used in a variety of applications including information compression, pattern mining, clustering and classification, facial recognition, missing data estimation, data-driven modelling and Galerkin projections. PCA aims to find an optimal set of basis vectors that captures energetically dominant features of the dataset. These basis vectors are also referred to as eigenfeatures or POD modes

or principal directions/components. The assumption is that a few of these modes are sufficient to capture all significant features of the dataset i.e., the data is highly correlated and inherently low rank. In many of these cases, the dataset is also large, often distributed over several computers and dense. For fluid-flow data, consisting of either measured or computed pressure, density or velocity at various spatial locations and several instants of time, the POD modes are used for identification and visualization of flow-structures, information compression or data-driven/reduced-order modelling[2]. In image processing, the data consists of several images and the eigenfeatures are used, for example, in facial classification and recognition [3, 4]. In computational biology, eigengenes and eigenarrays are used to model gene expression patterns [5, 6].

We use the following notation throughout the paper, unless otherwise specified. Lower case letters are used to denote scalars. Lower case bold-face letters are used to denote a vector. Upper case letters are used to denote a matrix. The i^{th} element of vector \mathbf{a} (bold font) is denoted as a_i (non-bold font). The element in the i^{th} row and j^{th} column of the matrix A is denoted by a_{ij} . \mathbf{a}^i denotes the i^{th} row vector and \mathbf{a}_j denotes the j^{th} column vector of matrix A . A_k denotes the best rank- k approximation of a matrix A and the approximation to A_k is denoted using tilde, as \tilde{A}_k . $|\mathbf{x}|$ denotes the norm of vector \mathbf{x} . $\|A\|_p$ denotes the p norm of matrix A .

Let D be the matrix that contains the data. In the case of images, each column of D corresponds to pixel values of an image. For fluid flow, each column of D contains spatially discretized values of the flow data at a particular instant of time (referred to as a “snapshot”). Therefore, each row represents the time evolution of the flow data at a particular spatial grid point. In the discussion that follows, we use the terms images and snapshots interchangeably. Let A denote the matrix obtained by mean-centering the entries of each row of D i.e., we subtract out the “mean face” or “the mean flow”. The element z_{ij} in $Z = AA^T$ is a measure of the average covariance between pixels or flow data values at various grid points. The eigenvector, \mathbf{u}_1 , of Z corresponding to the largest eigenvalue λ_1 is the first POD mode. It is the direction along which the energy in the projections of the mean-centered snapshots is maximised. The second mode is obtained by finding the direction orthogonal to \mathbf{u}_1 such that the energy of the projections in this direction is maximised. This is the eigenvector of Z corresponding to the next largest eigenvalue and so on.

The eigenvectors of Z are the left-singular vectors of A and can be obtained by computing the singular value decomposition (SVD) of A . Let $A = U\Sigma V^T$ be the SVD of A and $A_k = U_k \Sigma_k V_k^T$ be the matrix formed using the top k singular values and the corresponding singular vectors. It is well known that A_k is the best rank- k approximation to A in the sense that $\|A - A_k\|_p \leq \|A - B\|_p$, where B is any other matrix of rank at most k and $\|\cdot\|_p$ is any unitarily invariant norm (most often, $p = 2$ (spectral norm), F (Frobenius norm) are used). The matrix U_k contains the first k POD modes. For a dense $m \times n$ matrix, the computation of SVD is $O(mn\min(m, n))$. Since the data matrix is often very large, computing its SVD becomes impractical both in terms of memory and runtime. Therefore, it becomes attractive to find an approximation for A_k , \tilde{A}_k , such that the error is bounded and it can be obtained in a computationally efficient manner.

Approximate SVD algorithms can be classified broadly into two categories: random projection and sampling based algorithms or a combination of both. The error in the approximation can be either additive, which is of the form

$$\|A - \tilde{A}_k\|_p \leq \|A - A_k\|_p + O(\epsilon, k)\|A\|_p \quad (1)$$

or multiplicative where

$$\|A - \tilde{A}_k\|_p \leq (1 + O(\epsilon, k))\|A - A_k\|_p. \quad (2)$$

The random projection methods work by projecting either rows or columns of the matrix onto a random subspace [7, 8, 9]. The assumption is that a small number of randomly generated vectors are linearly independent with high probability and a projection of the rows/columns of A onto this random basis captures the dominant row/column subspace of A . Power iterations [7, 9] or subspace iterations [10] are additionally employed to improve the approximation, especially if the singular values decay slowly. The trade-off is between accuracy and run-time. The projection based methods have multiplicative error.

Sampling based algorithms have been used to find a smaller sketch of the matrix so that the rank- k approximation of the sketch, \tilde{A}_k , is approximately equal to A_k . The sketch is either a sparse version of the matrix [11] or it contains a subset of the rows and columns of the matrix that are chosen either deterministically or randomly based on a probability distribution. This distribution can be uniform [12] or non-uniform. Non-uniform probability distributions can then either be based on the row/column norms [13, 14, 1] or based on row/column leverage scores ([15]).

Achlioptas and McSherry [11] sparsify the matrix based on magnitude of the elements. The motivation behind this is to obtain an improvement in the runtime using sparse SVD solvers, while maintaining accuracy. Frieze *et al* [14] sample a subset of rows and columns to obtain a smaller matrix. The rows and columns are scaled to get an unbiased estimate and the SVD of the small matrix is used to compute \tilde{A}_k . Drineas *et al* [1] use the same sampling and scaling technique, but propose two pass-efficient algorithms - Linear time SVD(LTSVD) in which only columns are sampled and constant time SVD(CTSVD) that samples both columns and rows. Also, they have improved bounds for the error and based on their analysis, LTSVD requires $\Omega(k/\epsilon^2)$ columns while CTSVD samples $\Omega(k^2/\epsilon^4)$ columns and rows. In all these cases the error is additive.

Multiplicative error bounds can be obtained using adaptive sampling, which has several rounds of sampling based on row/column norms [16, 17]. Alternatively, sampling can be done using leverage scores [15, 18, 19] which are computed using the singular vectors or the pseudo-inverse of A , which in turn require its SVD. However, approximate leverage scores have been used [20], [21], but they too require either the SVD or QR decomposition of a smaller matrix to compute the scores. Leverage scores have also been used in the context of incremental/online SVDs in [22].

Menon and Elkan[23] have done experimental evaluations of some of the sampling and projection algorithms using MATLAB. They have evaluated the sparsifying technique of [11], LTSVD method proposed by [1] and the projection-based algorithms proposed in [8, 24, 9], in terms of runtime and accuracy for various sparse and dense datasets. Their results indicate that for dense datasets, the accuracy of the column sampling method, which has additive error bounds, is comparable to the projection methods that have multiplicative error bounds. It is only slightly worse for sparse datasets. Overall, they conclude that the column sampling method of [1] has low overheads and gives “excellent accuracy with low runtimes”. An additional advantage of sampling based methods is that they tend to retain sparsity, while projection based methods often convert a sparse matrix into a smaller, but dense matrix [21].

1.1 Our contributions

In this paper, we explore the sampling based techniques further. We start with the LTSVD and CTSVD algorithms proposed in [1] and discuss the advantages and limitations of the technique. We evaluated the algorithms based on the runtime, the accuracy of the eigenfeatures/POD modes and the accuracy of the subspaces spanned by the modes. The error bounds derived in [1] hold when sampling is done with replacement. Many data matrices

are “tall-and-skinny”, so that when the error parameters are tightened to improve accuracy, the number of columns sampled turns out to be a significant fraction of the total number of columns in the matrix. A similar limitation holds with row-sampling for “short and fat” matrices. In these cases, sampling with replacement leads to several columns/rows being sampled repeatedly. Since the computation of the SVD of tall-and-skinny matrices depends quadratically on the number of columns sampled, this incurs a runtime penalty. In this paper, we first show that with appropriate scaling, identical results can be obtained for the singular values and left-singular vectors, while retaining only distinct column and row indices. In this case, the right singular vectors of the sampled matrix obtained will not be the same as that computed in LTSVD or CTSVD. We derive a relationship between the right singular vectors computed using LTSVD/CTSVD and those computed by retaining only distinct columns/row indices. This scaling can be used for both dense and sparse matrices. It is independent of the probability distribution used to sample the matrix and can be used to improve performance whenever sampling is done with replacement.

Our results indicate that the POD modes as well as the subspaces often have a significant error, even when the error $\|A - \tilde{A}_k\|_F$ is well below theoretical bounds. To improve the accuracy of the POD modes or subspace spanned by the POD modes, we propose an iterative algorithm in which additional columns and rows are sampled in each iteration. Unlike the adaptive sampling method of [17], the approximate singular vectors are updated in each iteration using a previously proposed merge-and-truncate algorithm (MAT) [25]. The iteration is stopped when either the POD modes or the subspaces spanned by the modes converge. A more detailed comparison with the adaptive sampling algorithm is included in section 4. Although we have no theoretical bounds for the error, results on various datasets indicate that the POD modes are approximated with excellent accuracy. We explore two different sampling strategies in each iteration to obtain a robust algorithm with a good runtime improvement over computing a truncated SVD.

For large matrices that do not fit in the RAM or are distributed on several machines, one possibility is to partition the matrix. A sampling based algorithm can be used on each partition and the SVD can be incrementally updated using the MAT algorithm. There is no reason to expect that these algorithms have the same accuracy as a single sampling of the entire matrix. We evaluate experimentally the accuracy of incremental algorithm for a large dataset. Incremental algorithms have been used previously for streaming data [22], where randomized sampling and projection is used to get the approximate SVD of new batches of columns.

The paper is organised as follows: Section 2 describes the LTSVD and CTSVD algorithms of [1] and motivates our modifications to these algorithms. Section 3 describes and gives proofs for the unique sampling algorithms. Section 4 describes our two iterative algorithms. In section 5 we discuss the results of these algorithms as applied to different datasets. Section 6 concludes the paper.

2 Motivation

Linear and constant time SVD algorithms proposed in [1] are presented in this section. These algorithms obtain \tilde{A}_k by sampling a certain number of columns and/or rows of A using a sampling probability distribution based on L_2 norms of the columns and rows of the matrix. In this section, we describe the two algorithms and discuss the limitations of the algorithms.

2.0.1 Linear time SVD (LTSVD)

LTSVD samples c columns of A with replacement based on a predefined probability distribution. The sampled and scaled columns form the matrix C . The objective is to approximate A_k well using the SVD of C . The algorithm guarantees that, if

$$c \geq 4k\eta^2/(\beta\epsilon^2) \quad (3)$$

and the probability of sampling the i^{th} column is

$$p_i \geq \beta \frac{|\mathbf{a}_i|^2}{\|A\|_F^2}, \quad (4)$$

the inequality

$$\|A - \tilde{U}_k \tilde{U}_k^T A\|_F^2 \leq \|A - A_k\|_F^2 + \epsilon \|A\|_F^2 \quad (5)$$

holds with a probability of at least $(1 - \delta)$. Here, \tilde{U}_k is the matrix containing the first k left singular vectors of C and $\eta = 1 + \sqrt{(8/\beta) \log(1/\delta)}$ with $0 < \beta, \delta \leq 1$. The failure probability, δ , is the probability with which equation (5) fails to hold. ϵ is the error parameter where $\epsilon > 0$. The authors also have the corresponding results for the spectral norm. Throughout this paper, we have used the results for the Frobenius norm, with a failure probability rather than the bounds for the expected value. Algorithm 1 contains the pseudo-code for LTSVD.

Algorithm 1 LTSVD algorithm. Inputs: matrix $A \in \mathbb{R}^{m \times n}$, vector containing sampling probabilities \mathbf{p} , number of columns to be sampled c , and rank of approximation, k .

```

1: procedure LTSVD( $A, \mathbf{p}, k, c$ )
2:    $C \leftarrow \text{SAMPLE AND SCALE COLUMNS}(A, \mathbf{p}, c)$ 
3:    $\tilde{V} \tilde{\Sigma}^2 \tilde{V}^T \leftarrow \text{SVD}(C^T C)$   $\triangleright \tilde{V}, \tilde{\Sigma}$  are the right singular vectors and values of  $C$ 
4:    $\tilde{\mathbf{u}}_i \leftarrow C \tilde{\mathbf{v}}_i / \tilde{\sigma}_i$  where  $i = 1, 2, \dots, l$  and  $l = \min(k, r)$ ;  $r$ : rank of  $C$ 
5:   return  $\tilde{\mathbf{u}}_i, \tilde{\sigma}_i$  where  $i = 1, 2, \dots, l$ 
6: end procedure
7: procedure SAMPLE AND SCALE COLUMNS( $A, \mathbf{p}, c$ )
8:   for  $i \leftarrow 1, 2, \dots, c$  do
9:     Pick  $s_i \in \{1, 2, \dots, n\}$  with probability  $\Pr[s_i = \alpha] = p_\alpha, \alpha = 1, 2, \dots, n$ 
10:     $\mathbf{c}_i \leftarrow \mathbf{a}_{s_i} / \sqrt{c p_{s_i}}$ 
11:   end for
12:   return  $C$ 
13: end procedure

```

2.0.2 Constant time SVD (CTSVD)

CTSVD samples c columns of A , scales them and forms the matrix C . It then samples w rows from C based on the row norms of C and scales them appropriately to form the matrix W . As in LTSVD, sampling is done with replacement. First, the right singular vectors, $\tilde{\mathbf{v}}_i$, of W are computed by finding the SVD of $W^T W$. \tilde{U}_l , matrix containing $\tilde{\mathbf{u}}_i$ where $1 \leq i \leq l$, is then computed as $\tilde{\mathbf{u}}_i = C \tilde{\mathbf{v}}_i / \tilde{\sigma}_i$ where $l = \min(k, \max(r : \tilde{\sigma}_r^2 > \gamma \|W\|_F^2))$ with $\gamma = \epsilon/(100k)$.

If

$$c, w \geq k^2 \eta^2 / \epsilon^4, \quad (6)$$

and sampling probability distribution for columns and rows is given by

$$p_i = \frac{|\mathbf{a}_i|^2}{\|A\|_F^2}, \quad (7)$$

$$q_j = \frac{|\mathbf{c}^j|^2}{\|\mathbf{C}\|_F^2}, \quad (8)$$

the inequality,

$$\|A - \tilde{U}_l \tilde{U}_l^T A\|_F^2 \leq \|A - A_k\|_F^2 + \epsilon \|A\|_F^2 \quad (9)$$

holds with probability of at least $(1 - \delta)$ where $\eta = 1 + \sqrt{8 \log(2/\delta)}$, the error parameter, $\epsilon > 0$, and the failure probability, $0 < \delta \leq 1$. Algorithm 2 gives the pseudo-code for CTSVD. Note that since the left singular vectors, $\tilde{\mathbf{u}}_i$, are computed using the right singular vectors

Algorithm 2 CTSVD Algorithm. Inputs: matrix $A \in \mathbb{R}^{m \times n}$, vector containing sampling probabilities for column sampling \mathbf{p} , number of columns c and rows w to be sampled, and rank of approximation, k

```

1: procedure CTSVD( $A, \mathbf{p}, k, c, w$ )
2:    $C \leftarrow \text{SAMPLE AND SCALE COLUMNS}(A, \mathbf{p}, c)$ 
3:    $W \leftarrow \text{SAMPLE AND SCALE ROWS}(C, w)$ 
4:    $\tilde{V} \tilde{\Sigma}^2 \tilde{V}^T \leftarrow \text{SVD}(W^T W)$ 
5:    $\gamma \leftarrow \epsilon / (100k)$ 
6:    $l \leftarrow \min(k, \max(r : \tilde{\sigma}_r^2 \geq \gamma \|W\|_F^2))$ 
7:    $\tilde{\mathbf{u}}_i \leftarrow C \tilde{\mathbf{v}}_i / \tilde{\sigma}_i$  where  $i = 1, 2, \dots, l$ 
8:   return  $\tilde{\mathbf{u}}_i, \tilde{\sigma}_i$  where  $i = 1, 2, \dots, l$ 
9: end procedure
10: procedure SAMPLE AND SCALE ROWS( $C, w$ )
11:    $q_j \leftarrow |\mathbf{c}^j|^2, j = 1, 2, \dots, m$ 
12:    $q_j \leftarrow q_j / \sum_{h=1}^m q_h$ 
13:   for  $j \leftarrow 1, 2, \dots, w$  do
14:     Pick  $\hat{s}_j \in \{1, 2, \dots, m\}$  with probability  $\Pr[\hat{s}_j = \alpha] = q_\alpha, \alpha = 1, 2, \dots, m$ 
15:      $\mathbf{w}^j \leftarrow \mathbf{c}^{\hat{s}_j} / \sqrt{w q_{\hat{s}_j}}$ 
16:   end for
17:   return  $W$ 
18: end procedure

```

of W instead of C (see Algorithm 2, line 7), \tilde{U}_l may not be an orthogonal matrix.

2.1 Results

LTSVD and CTSVD (Algorithms 1 and 2, respectively) were run with different parameter values on the following datasets.

1. Faces data from [26], a collection of 400 images from 40 subjects, each of size 112×92 . The matrix is of size 10304×400 . Each column in the matrix consists of values of a single image. This dataset will be referred to as Faces dataset in the paper. This dataset was also used by [23] for evaluation of the algorithms.
2. A matrix of size 132098×1024 consisting of 1024 snapshots of velocity vector data of a flow generated using a CFD simulation on a grid of size 257×257 . Each column of the matrix contains the x and y components of the velocity. It will be referred as V_{2D} .
3. 2414 images of 38 subjects cropped to show only the face of the subject in different illumination conditions from [27]. The images are of size 192×168 giving a matrix of dimensions 32256×2414 , stacked similar to the Faces dataset. This dataset is referred to as cropped Yale faces (CYF).

4. Faces data from [28], a collection of 16128 images from 28 subjects in different poses and illumination conditions. Each image is of size 480×640 that are stacked similar to the Faces dataset. 18 of the 16128 images in the database were discarded since they were corrupted. This dataset is referred to as Yale faces (YF) and is of size 307200×16110 .

All the datasets are mean-centered row-wise.

Fig. 1 shows the first 20 singular values for these datasets. V_{2D} has a dominant singular value, followed by a sharp decay. The most gradual decay of singular values is for the YF dataset, where the first two modes capture only 30% of the energy. For CYF the first two singular values are very close. For all datasets, but especially for CYF, there is a clustering of the singular values beyond the first ten values. Note that the singular values of V_{2D} is plotted on a log scale, while others are on a linear scale.

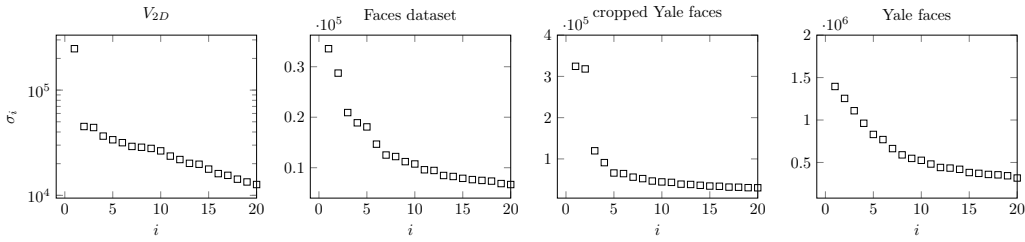


Figure 1: First 20 singular values of datasets considered.

It is difficult to fix values of the error parameters ϵ and δ for the two algorithms. Instinctively, we would like it to be small (< 1). However, since the number of columns sampled depends inversely on powers of ϵ , it increases rapidly and often exceeds the number of columns in the matrix. This limits the parameter values that can be used. Since the datasets in many applications turn out to be tall-and-skinny, sampling of rows is not a limitation. To get some representative results, we looked at results for three cases namely, C1: $c \approx n$ except for the YF dataset, where it is lower, C2: $c \approx n/2$ (lower for CYF), and C3: $c \ll n$ (higher for YF). For V_{2D} , Faces and CYF, we used $k = 10, 5, 2$ for the three cases C1, C2, and C3 respectively. Since YF is a larger dataset, with a more gradual decay of singular values, we used $k = 20, 10, 5$ for the three cases. For these cases, c, k, ϵ, δ are shown in Tables 1 and 2. It is seen that very often ϵ is around one, suggesting liberal upper bounds.

In our implementation, the random number generator provided by the *numpy* package in Python3 was used.

In all cases, we found that the error in approximating A_k is well below the theoretical error bound for the respective algorithms. Fig. 2 shows the percentage error in the singular values. In the case of CTSVD C1, we could not obtain 10 values with the filter and the values plotted are obtained without the filter. It is seen that the error is less than 5% for CYF and YF. The two dominant singular values are captured accurately even when the error parameter values are close to one. The error is slightly larger for V_{2D} and Faces dataset, but is still less than 20%, except for CTSVD (C3) for the V_{2D} dataset.

For many applications in fluid flow and in gene expression modelling, it is the POD modes rather than the singular values that are important. A measure of the accuracy of the POD modes is the cosine similarity between the approximate mode (\tilde{u}_i) and the one obtained using a truncated SVD of the entire dataset (u_i). Fig. 3 shows the angle between

Table 1: Number of columns sampled (c) by LTSVD and number of columns (c) and rows (w) sampled by CTSVD when run on different datasets with different parameter values as set in Table 2.

Case	LTSVD				CTSVD			
	V_{2D} c	Faces c	CYF c	YF c	V_{2D} $c = w$	Faces $c = w$	CYF $c = w$	YF $c = w$
C1	1016	389	2400	9924	1022	395	2316	10488
C2	561	226	561	8334	869	282	869	8421
C3	44	44	44	4167	55	55	55	4978

Table 2: Parameter values (k, ϵ, δ) used in LTSVD and CTSVD algorithms for various datasets

Case	V_{2D} k, ϵ, δ	Faces k, ϵ, δ	CYF k, ϵ, δ	YF k, ϵ, δ
LTSVD				
C1	10, 0.7, 0.45	10, 0.75, 0.8	10, 0.46, 0.44	20, 0.35, 0.35
C2	5, 1, 0.1	5, 0.75, 0.75	5, 1, 0.1	10, 0.3, 0.25
C3	2, 1, 0.8	2, 1, 0.8	2, 1, 0.8	5, 0.3, 0.25
CTSVD				
C1	10, 1.04, 0.94	10, 1.3, 1	10, 0.9, 0.7	20, 0.83, 0.9
C2	5, 1, 0.1	5, 1, 0.1	5, 1, 1	10, 0.62, 0.9
C3	2, 1, 0.8	2, 1, 0.8	2, 1, 0.8	5, 0.5, 0.9

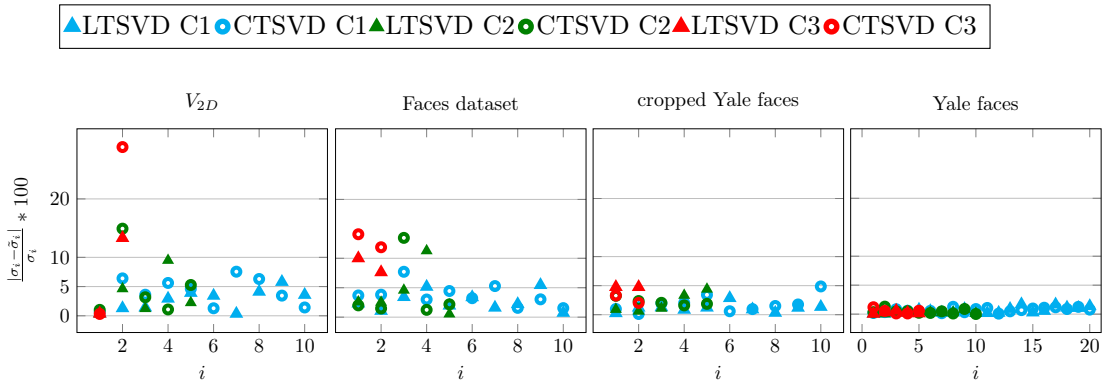


Figure 2: Percentage error in the singular values of different datasets computed by LTSVD (Algorithm 1) and CTSVD (Algorithm 2) for different parameter values, as given in Table 2.

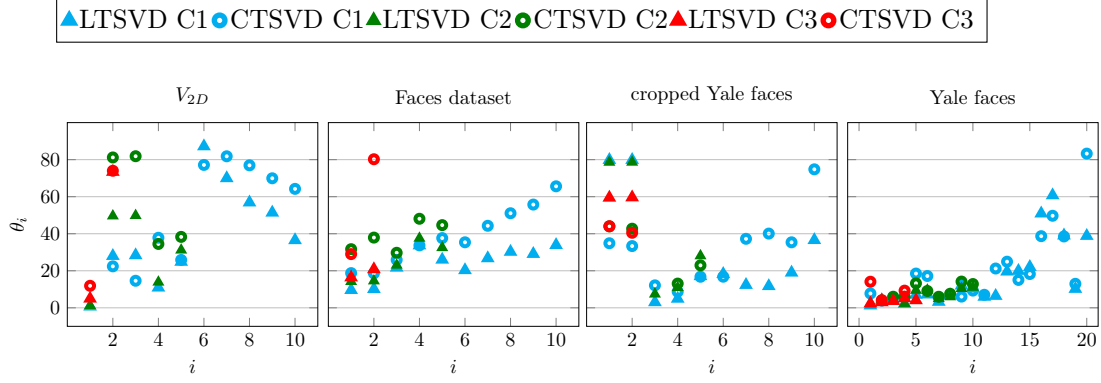


Figure 3: First k mode angles, θ_i , for different datasets computed by LTSVD (Algorithm 1) and CTSVD (Algorithm 2) for different parameter values, as given in Table 2.

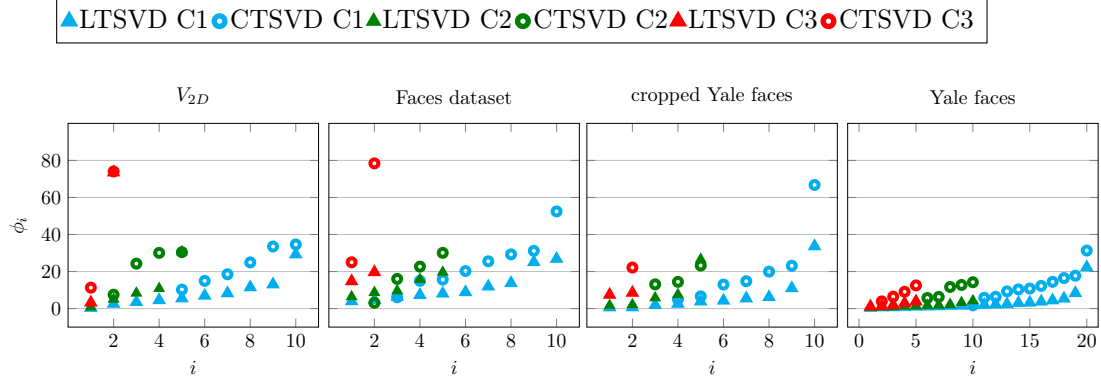


Figure 4: First k principal angles, ϕ_i , for different datasets computed by LTSVD (Algorithm 1) and CTSVD (Algorithm 2) for different parameter values, as given in Table 2.

the two, computed as

$$\theta_i = \arccos(|\mathbf{u}_i^T \tilde{\mathbf{u}}_i|) \frac{180}{\pi} \quad (10)$$

The absolute value of $\mathbf{u}_i^T \tilde{\mathbf{u}}_i$ is taken in equation (10) so that $0^\circ \leq \theta_i \leq 90^\circ$ where $\theta_i = 0^\circ$ denotes that $\tilde{\mathbf{u}}_i$ and \mathbf{u}_i are equal up to sign ($\tilde{\mathbf{u}}_i = \pm \mathbf{u}_i$). We refer to these angles as “mode angles”. It can be seen from Fig. 3 that the accuracy of the modes is best for YF where nearly ten modes are approximated well, possibly because the energy is more evenly distributed among the modes. For the other datasets, the modes are approximated very poorly even for LTSVD C1, for which $c \approx n$. In the case of CYF, the first two modes are very poorly approximated.

The mode angles are known to be sensitive to clustering of singular values. In the limiting case when the singular values are identical, it is only the eigenspace that matters and not the eigenvectors. Also, for applications such as facial recognition, it is the space spanned by the the modes rather than the modes themselves that are of interest. For this reason, we also measure the accuracy of the subspaces spanned by k singular vectors rather than the accuracy of each mode. A measure of this accuracy is the principal or canonical

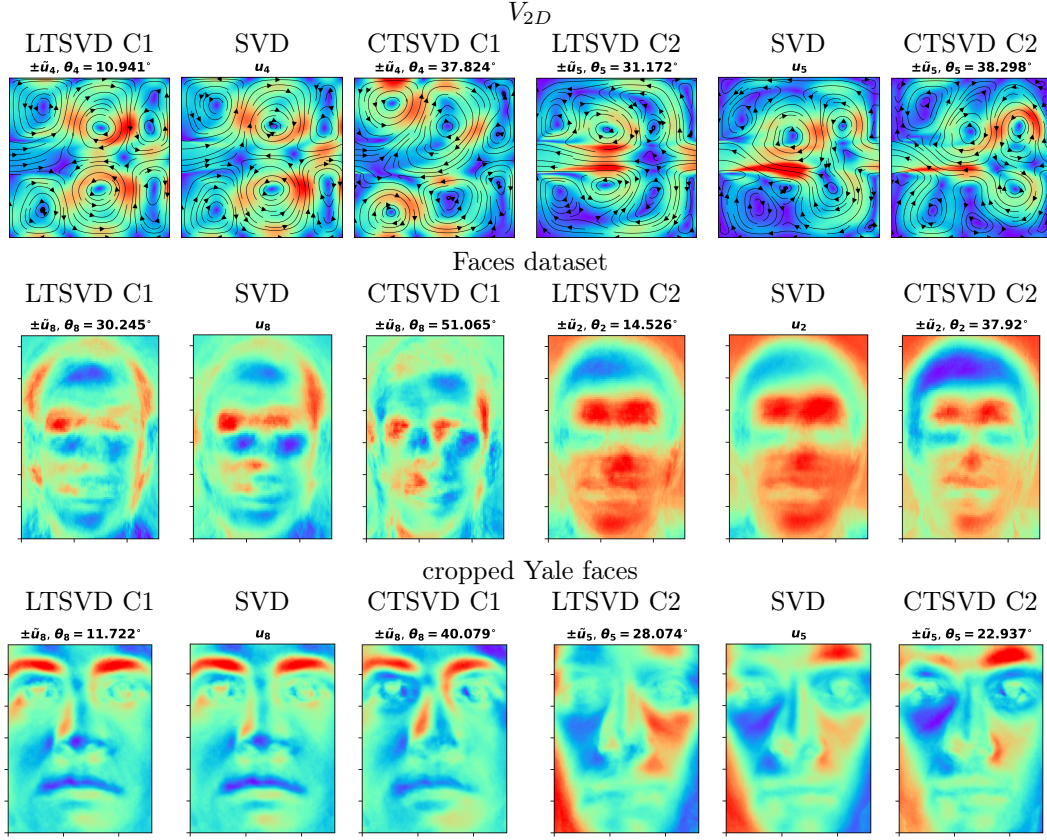


Figure 5: POD modes of various datasets computed by SVD, LTSVD (Algorithm 1) and CTSVD (Algorithm 2). POD mode of V_{2D} consists of both the x and y components of velocity vector at each point in space. The color at each point denotes the magnitude of this vector at that point. Streamlines shown, denote the direction of the flow captured by the POD mode.

angles between the subspaces, whose cosines are the singular values of $\tilde{U}_k^T U_k$ [29]. Fig. 4 shows the k principal angles, ϕ_i , between the two k -dimensional subspaces. Although the accuracy of the subspace is better than the modes themselves, the error increases as k increases and in some cases, there is significant error even for $c \approx n$. The first two principal angles for CYF match well, indicating that the subspace is captured more accurately than the modes themselves. In general for the datasets considered, LTSVD always gives better approximations than CTSVD and the accuracy is, once again, best for YF.

In order to see the significance of the mode angles, few POD modes from the datasets are plotted in Fig. 5. It is seen from the images that when the angle is large, the corresponding features are distorted or completely absent in some cases. Generally, for the datasets we have looked at, POD modes that have a deviation of around $10 - 20^\circ$ seem to capture the features of the actual POD modes well- i.e. with less or no visually apparent distortions.

From Fig. 3 and Fig. 4, it is surprising to see that for all datasets, the error in the modes as well as the subspace spanned by the modes is significant even with $c \approx n$. This is because sampling is done with replacement, which means that some of the columns are sampled more than once, while others are not sampled at all. Table 3 shows the number of distinct column and row indices sampled in each case. It can be seen that when $c \approx n$, there is a $1.3 - 2.2\times$ overhead due to repeated sampling of the same columns, while for $c \ll n$, nearly all the columns are distinct. Nearly all rows are distinct since $w \ll m$ in all cases. Since the runtime depends quadratically on the number of columns in the matrix, this overhead results in a nearly $1.5 - 4\times$ increase in the runtime. The second issue is the accuracy of the modes/subspaces, which seems sensitive to the singular value profile and degrades for larger k values. We address these two issues in the following sections.

Table 3: Number of distinct columns, g , sampled by LTSVD and number of distinct columns, g , and rows, h , sampled by CTSVD for different parameter values when run on various datasets.

Case	LTSVD		CTSVD			LTSVD		CTSVD		
	c	g	$c = w$	g	h	c	g	$c = w$	g	h
V_{2D}						faces				
C1	1016	460	1022	457	1008	389	246	395	244	385
C2	561	314	869	401	861	226	170	282	198	279
C3	44	41	55	52	55	44	40	55	54	55
CYF						YF				
C1	2400	1412	2316	1394	2253	9924	7073	10488	7376	10103
C2	561	482	869	716	857	8334	6252	8421	6294	8199
C3	44	43	55	55	55	4167	3608	4978	4178	4892

3 Linear and constant time SVD with distinct columns and rows

In this section, we will prove that the repeated columns and/or rows sampled in LTSVD and CTSVD can be removed without changing the singular values and left singular vectors computed by LTSVD and CTSVD algorithms provided the columns/rows are appropriately

scaled. We also derive a relationship between the right singular vectors with and without repeated row/columns.

Consider the following matrix,

$$A_{m \times n} = [\mathbf{a}_1 \quad \mathbf{a}_2 \quad \cdots \quad \mathbf{a}_n] \quad (11)$$

where $\mathbf{a}_i, (i = 1, 2, \dots, n)$ are column vectors. Let C be the matrix containing c columns sampled from A with replacement, of which there are g distinct columns. Let $\mathbf{I}_d = \{d_1, d_2, \dots, d_g\}$ be the indices of these distinct columns, each \mathbf{a}_{d_i} occurring t_i times in an arbitrary order in C . Based on Algorithm 1, the columns of C are constructed as

$$C_{m \times c} = [\mathbf{c}_j]_{j=1}^c = \left[\frac{1}{\sqrt{cp_{d_i}}} \mathbf{a}_{d_i} \right]; \quad d_i \in \mathbf{I}_d \quad (12)$$

Let D be the matrix containing only distinct columns of C . Let the column of D with index d_i be scaled as follows.

$$D_{m \times g} = [\mathbf{d}_i]_{i=1}^g = \left[\sqrt{\frac{t_i}{cp_{d_i}}} \mathbf{a}_{d_i} \right]_{i=1}^g \quad (13)$$

Clearly,

$$CC^T = \sum_{i=1}^g \frac{t_i}{cp_{d_i}} \mathbf{a}_{d_i} \mathbf{a}_{d_i}^T = DD^T. \quad (14)$$

This shows that the eigenvalues and eigenvectors of CC^T are the same as those of DD^T . Hence, the non-zero singular values and the corresponding left singular vectors (up to a multiplicative factor of -1) of C and D are also identical i.e. $\Sigma_C = \Sigma_D$ and $U_C = U_D$ where Σ_C/Σ_D contains only the non-zero singular values of the corresponding matrix.

The two right singular vectors, V_C and V_D , are not the same, but V_D can be derived from V_C as follows. Without loss of generality, assume that the repeated columns in C are grouped together forming the matrix B . Hence, B can be written as

$$B_{m \times c} = \left[\underbrace{\frac{1}{\sqrt{cp_{d_1}}} \mathbf{a}_{d_1} \cdots}_{\text{occurring } t_1 \text{ times}} \quad \underbrace{\frac{1}{\sqrt{cp_{d_2}}} \mathbf{a}_{d_2} \cdots}_{\text{occurring } t_2 \text{ times}} \quad \underbrace{\frac{1}{\sqrt{cp_{d_g}}} \mathbf{a}_{d_g} \cdots}_{\text{occurring } t_g \text{ times}} \right] \quad (15)$$

B is a column-permuted matrix of C . If P denotes the permutation matrix, $B = CP$. Let $C = U_C \Sigma_C V_C^T$ and $B = U_B \Sigma_B V_B^T$ denote the SVDs of C and B respectively. Therefore,

$$B = CP = U_C \Sigma_C V_C^T P = U_B \Sigma_B V_B^T \quad (16)$$

Since the permutation matrix is orthogonal, we have $V_B = P^T V_C$.

V_B can also be obtained from the right singular vectors of D as follows. Define a matrix T as

$$T = \left[\begin{array}{ccccccccc} \frac{1}{\sqrt{t_1}} & \cdots & \frac{1}{\sqrt{t_1}} & 0 & \cdots & & & & \\ 0 & \cdots & & \frac{1}{\sqrt{t_2}} & \cdots & \frac{1}{\sqrt{t_2}} & \cdots & 0 & \cdots \\ & & \ddots & 0 & \cdots & 0 & & & \ddots \\ & & & & \ddots & & & & \\ & & & & & & \frac{1}{\sqrt{t_g}} & \cdots & \frac{1}{\sqrt{t_g}} \\ \underbrace{\hspace{1.5cm}}_{\text{occurring } t_1 \text{ times}} & \underbrace{\hspace{1.5cm}}_{\text{occurring } t_2 \text{ times}} & \cdots & \underbrace{\hspace{1.5cm}}_{\text{occurring } t_g \text{ times}} \end{array} \right]. \quad (17)$$

Note that the rows of T are orthogonal i.e., $TT^T = I$ and $B = DT$. Therefore, the SVDs of B and D are related as follows

$$B = U_B \Sigma_B V_B^T = U_D \Sigma_D V_D^T T \quad (18)$$

Since the rows of T are orthogonal, the columns of $T^T V_D$ are orthogonal. Hence, the left singular vectors B and D are identical and the right singular vectors are related as $V_B = T^T V_D$.

From equations (16) and (18),

$$C = U_C \Sigma_C V_C^T = U_D \Sigma_D V_D^T T P^T = D T P^T. \quad (19)$$

Hence, C and D have the same singular values and left singular vectors and their right singular vectors are related as $V_C = P T^T V_D$. Since D is a smaller matrix, LTSVD can be made computationally more efficient, while giving exactly the same results. The first procedure in Algorithm 3 details the steps in the modified sample and scale algorithm. We call the revised algorithm LTSVD_US.

A similar procedure can be used in the case of column and row sampling. CTSVD_US uses the second procedure in Algorithm 3 to additionally sample and scale rows. We now prove that CTSVD_US will give the same results as CTSVD. Since $C C^T = D D^T$, row norms of C and D are identical and $\|C\|_F = \|D\|_F$. Therefore, the probability distribution used for sampling rows is the same irrespective of whether D or C is used to obtain the sampled rows. Let M be an indicator matrix that chooses rows from C or D . M can be written as follows.

$$m_{ij} = \begin{cases} 1, & \text{if row } j \text{ is sampled in the } i^{\text{th}} \text{ round of sampling,} \\ 0, & \text{otherwise.} \end{cases} \quad (20)$$

If the number of rows sampled is w , M is a $w \times m$ matrix and $W = M C$ is matrix containing the rows sampled from C . Once again, the sampling is done with replacement. Using equation (19), we have

$$W = M D T P^T. \quad (21)$$

Let $X = M D$ contain rows sampled from D using M . It is clear that

$$\begin{aligned} W W^T &= M D T P^T P T^T D^T M^T \\ &= M D D^T M^T = X X^T \end{aligned} \quad (22)$$

Therefore, the non-zero singular values and the corresponding left singular vectors of W and X are equal. Since $W = X T P^T$, the right singular vectors are related as follows.

$$V_W = P T^T V_X \quad (23)$$

Both W and X potentially contain more than one copy of the sampled rows. Define \hat{T} as follows.

$$\hat{T} = \begin{bmatrix} \underbrace{\frac{1}{\sqrt{\hat{t}_1}} \cdots \frac{1}{\sqrt{\hat{t}_1}}}_{\text{occurring } \hat{t}_1 \text{ times}} & 0 & \cdots & 0 & \cdots & \cdots & \cdots & \cdots & \cdots \\ 0 & \underbrace{\frac{1}{\sqrt{\hat{t}_2}} \cdots \frac{1}{\sqrt{\hat{t}_2}}}_{\text{occurring } \hat{t}_2 \text{ times}} & \cdots & \frac{1}{\sqrt{\hat{t}_2}} & \cdots & \frac{1}{\sqrt{\hat{t}_2}} & \cdots & 0 & \cdots \\ & & \ddots & 0 & \cdots & 0 & & & \ddots \\ & & & & \ddots & & & \frac{1}{\sqrt{\hat{t}_h}} & \cdots & \frac{1}{\sqrt{\hat{t}_h}} \\ & & & & & & & \underbrace{\frac{1}{\sqrt{\hat{t}_h}} \cdots \frac{1}{\sqrt{\hat{t}_h}}}_{\text{occurring } \hat{t}_h \text{ times}} \end{bmatrix}. \quad (24)$$

where h is the number of distinct rows that were sampled and \hat{t}_i is the number of occurrences of row with index \hat{d}_i in X . Following a similar procedure, we first permute rows of X so

that rows that have the same index are grouped together. Let \hat{P} denote the permutation matrix. Define a matrix Y that contains distinct rows of X , scaled as follows.

$$Y_{h \times g} = [\mathbf{y}^i]_{i=1}^h = \left[\sqrt{\frac{\hat{t}_i}{wp_{\hat{d}_i}}} \mathbf{x}_{\hat{d}_i} \right]_{i=1}^h \quad (25)$$

It is clear that

$$\hat{T}^T Y = \hat{P} X \quad (26)$$

Since $\hat{T}\hat{T}^T = I$ and \hat{P} is orthogonal, $Y^T Y = X^T X$. Hence the non-zero singular values and the corresponding right singular vectors of Y and X are equal. That is

$$\sigma_{Y,i} = \sigma_{X,i}, \quad \mathbf{v}_{Y,i} = \mathbf{v}_{X,i}, \quad i = 1, 2, \dots, h \quad (27)$$

In CTSVD_US, the approximate left singular vectors of A are obtained using

$$\tilde{\mathbf{u}}_i = \frac{D\mathbf{v}_{Y,i}}{\sigma_{Y,i}} = \frac{D\mathbf{v}_{X,i}}{\sigma_{X,i}} \quad (28)$$

Using Algorithm 2 and equations (19) and (23), the left singular vectors in CTSVD are computed as

$$\tilde{\mathbf{u}}_i = \frac{C\mathbf{v}_{W,i}}{\sigma_{W,i}} = \frac{DTPT^T \mathbf{v}_{W,i}}{\sigma_{W,i}} = \frac{D\mathbf{v}_{X,i}}{\sigma_{X,i}} \quad (29)$$

From equations (28) and (29), it can be seen that $\tilde{\mathbf{u}}_i$ computed by CTSVD and CTSVD_US are identical.

In summary, removing the duplicates and scaling the distinct columns and/or rows with the square root of number of occurrences of each sampled column and/or rows respectively, gives the same singular values and left singular vectors as the LTSVD and CTSVD algorithms. The modified algorithms, LTSVD_US and CTSVD_US, use the revised sample and scale algorithms detailed in Algorithm 3. Note that this revised scaling is completely independent of the sampling probability distribution.

4 Iterative Sampling

As discussed in section 2, the accuracy of the modes and subspaces spanned by the modes is poor even when the number of sampled columns is almost the same as the number of columns in the matrix. In the literature, an adaptive sampling algorithm [17] has been proposed to improve the accuracy of subspaces obtained using sampling algorithms. The steps involved are as follows

1. Sample k rows from A based on the approximate volume sampling (see [17] for details) and compute the basis, Q , spanning these rows.
2. Find the space orthogonal to the space spanned by these basis vectors, $E = A - AQQ^T$.
3. Sample s rows from A based on row norms of E and compute Q , the basis spanning all sampled rows.
4. Repeat from (2) for $(k+1)\log_2(k+1)$ times.

Algorithm 3 Inputs: matrix $A \in \mathbb{R}^{m \times n}$, number of columns to be sampled c and rank of approximation, k , ($1 \leq k \leq c$).

```

1: procedure SAMPLE AND SCALE UNIQUE COLUMNS( $A, p, c$ )
2:    $\mathbf{I}_s \leftarrow s_i \in \{1, 2, \dots, n\}$  with probability  $\Pr[s_i = \alpha] = p_\alpha, \alpha = 1, 2, \dots, n$ 
3:    $\mathbf{I}_d \leftarrow s_i : \forall \text{ distinct } s_i \in \mathbf{I}_s$ 
4:    $g \leftarrow \text{card}(\mathbf{I}_d)$  ▷ Cardinality of the set
5:    $\mathbf{t} \leftarrow \{t_{d_i}, \text{ number of occurrences in } \mathbf{I}_s \text{ of column with index } d_i \in \mathbf{I}_d\}$ 
6:    $\mathbf{c}_i \leftarrow \mathbf{a}_{d_i} \sqrt{t_{d_i}/(cp_{d_i})}$ , where  $d_i \in \mathbf{I}_d$  and  $i = 1, 2, \dots, g$ 
7:   return  $C$ 
8: end procedure
9: procedure SAMPLE AND SCALE UNIQUE ROWS( $C, w$ )
10:   $q_j \leftarrow |\mathbf{c}^j|^2, j = 1, 2, \dots, m$ 
11:   $q_j \leftarrow q_j / \sum_{h=1}^m q_h$ 
12:   $\hat{\mathbf{I}}_s \leftarrow \hat{s}_j \in \{1, 2, \dots, m\}$  with probability  $\Pr[\hat{s}_j = \alpha] = q_\alpha, \alpha = 1, 2, \dots, m$ 
13:   $\hat{\mathbf{I}}_d \leftarrow \hat{s}_j : \forall \text{ distinct } \hat{s}_j \in \hat{\mathbf{I}}_s$ 
14:   $h \leftarrow \text{card}(\hat{\mathbf{I}}_d)$ 
15:   $\hat{\mathbf{t}} \leftarrow \{\hat{t}_{\hat{d}_i}, \text{ number of occurrences in } \hat{\mathbf{I}}_s \text{ of row with index } \hat{d}_i \in \hat{\mathbf{I}}_d\}$ 
16:   $\mathbf{w}^i \leftarrow \mathbf{c}^{\hat{d}_i} \sqrt{\hat{t}_{\hat{d}_i}/(wq_{\hat{d}_i})}$ , where  $\hat{d}_i \in \hat{\mathbf{I}}_d$  and  $i = 1, 2, \dots, h$ 
17:  return  $W$ 
18: end procedure

```

In each round $2k$ rows are sampled, except for the last round where $16k/\epsilon$ rows are sampled. For $k = 10$ and $\epsilon = 0.5$, we would need 38 rounds of sampling and 1060 rows will be sampled to find the basis. Once the iteration is over, Q is an approximation to the basis for the row space. To obtain the approximate left-singular vectors, we need to additionally find the SVD of AQ . For the V_{2D} dataset, we see that AQ is approximately the same size as A and it is larger for the Faces dataset (for which you anyway cannot get more than 400 basis vectors). However, the advantage of this method is that (a) the error bound is multiplicative and (b) it is efficient as long as the number of basis vectors in Q is much less than n . Therefore, the algorithm can be made more efficient if there is some pruning of basis vectors in Q in each iteration, depending on whether it belongs to the dominant subspace or not.

Since we are looking to improve the accuracy of the left-singular vectors, we would like to have several rounds of column or column and row sampling rather than just row sampling. In each round, we would also like to prune the basis vectors that are not in the dominant subspace. Also, we would like to stop the iteration when the additional sampling does not improve the quality of either the modes or the subspace spanned by the modes. In order to do this we need an estimate of the POD modes in each iteration and we need an updating algorithm so that the SVD can be updated in each iteration. For this, we use the merge-and-truncate (MAT) algorithm proposed in [25], which is a computationally efficient and generalised version of the algorithm in [30].

We first outline the MAT algorithm and follow it up with a description of the iterative algorithm.

4.1 Merge and truncate (MAT) Algorithm

Let A be a matrix of size $m \times n$ that consists of sub-matrices X and Y containing n_1 and n_2 columns respectively, where $n = n_1 + n_2$. Assume that the rank- l approximations of X

and Y are $U_{1l}\Sigma_{1l}V_{1l}^T$ and $U_{2l}\Sigma_{2l}V_{2l}^T$. The rank- l approximation of A , \tilde{A}_l , can be computed from the individual SVDs by first merging the two SVDs and then truncating it to a rank- l approximation as follows. The component of U_{2l} orthogonal to U_{1l} is $U_t = U_{2l} - U_{1l}(U_{1l}^T U_{2l})$. If $U_t = U_o R$ is the corresponding QR decomposition, we have

$$\begin{aligned} \begin{bmatrix} X & Y \end{bmatrix} &\approx \begin{bmatrix} U_{1l} & U_o \end{bmatrix} \begin{bmatrix} \Sigma_{1l} & (U_{1l}^T U_{2l})\Sigma_{2l} \\ \mathbf{0} & \Sigma_{2l} R \end{bmatrix} \begin{bmatrix} V_{1l}^T & \mathbf{0} \\ \mathbf{0} & V_{2l}^T \end{bmatrix} \\ &= \begin{bmatrix} U_{1l} & U_o \end{bmatrix} E \begin{bmatrix} V_{1l}^T & \mathbf{0} \\ \mathbf{0} & V_{2l}^T \end{bmatrix} \end{aligned} \quad (30)$$

Now E is a much smaller $(2l) \times (2l)$ matrix. If $E = U_E \Sigma_E V_E^T$, we get

$$\begin{aligned} \begin{bmatrix} X & Y \end{bmatrix} &\approx \begin{bmatrix} U_{1l} & U_o \end{bmatrix} U_E \Sigma_E V_E^T \begin{bmatrix} V_{1l}^T & \mathbf{0} \\ \mathbf{0} & V_{2l}^T \end{bmatrix} \\ &= U \Sigma V^T \end{aligned} \quad (31)$$

where $U = \begin{bmatrix} U_{1l} & U_o \end{bmatrix} U_E$, $\Sigma = \Sigma_E$ and $V = V_E \begin{bmatrix} V_{1l}^T & \mathbf{0} \\ \mathbf{0} & V_{2l}^T \end{bmatrix}$. These singular values and vectors are once again truncated to get \tilde{A}_l . As discussed in [25], the MAT algorithm results in a significant speedup over computing the full SVD and then truncating it to a rank- l approximation. To make sure that the overall error is approximately the same as for LTSVD_US or CTSVD_US algorithms, the error due to the MAT algorithm must be significantly lower. Experiments over various data sets indicate that $l \approx 3k$ is sufficient. Algorithm 4 details the steps involved.

Algorithm 4 Pseudocode for block merge algorithm: merges left/right singular vectors of two adjacent blocks. Inputs: $U_1 \in \mathbb{R}^{m_1 \times n_1}$, $U_2 \in \mathbb{R}^{m_1 \times n_2}$, and truncation parameter $l \in \mathbb{N}$

- 1: **procedure** BLOCK_MERGE($U_1, \Sigma_1, U_2, \Sigma_2, l$)
 - 2: $U_{1l}, \Sigma_{1l}, U_{2l}, \Sigma_{2l} \leftarrow \text{Truncate}(U_1, \Sigma_1, U_2, \Sigma_2)$ retaining only l values
 - 3: Use equations (30) and (31) to find U and Σ
 - 4: $l \leftarrow \min(l, \max(r : \tilde{\sigma}_r \neq 0))$
 - 5: Truncate U and Σ retaining only l values
 - 6: **return** U, Σ
 - 7: **end procedure**
-

4.2 Iterative column and row sampling algorithm

We use the following steps in our iteration

1. Sample c columns of A with replacement based on column norms. Find distinct columns, form the matrix C and compute SVD of C . Truncate to retain l POD modes \tilde{U}_l . Matrix D contains the unsampled columns of A .
2. Sample c columns of D with replacement, using a uniform distribution ($S1$) or using a probability distribution based on column norms of the orthogonal component $D - \tilde{U}_l \tilde{U}_l^T D$ ($S2$). Note that the sampling strategy $S2$ is the same as that in the adaptive sampling algorithm.
3. Find distinct columns, compute SVD of the new columns and merge with the previously computed SVD using the MAT algorithm. Update D .

4. Find the angle between the current and newly computed k left singular vectors or the principal angles between the subspaces. If any one of the angles is greater than the desired value, continue the iteration.

Algorithm 5 Iterative SVD algorithm with column sampling; Inputs: matrix $A \in \mathbb{R}^{m \times n}$, sampling probability \mathbf{p} , number of columns to be sampled c (Equation (3)), rank of approximation, k , rank of matrices after BLOCK MERGE, l , and cosine similarity between POD modes computed in successive iterations, τ where $0 < \tau \leq 1$.

```

1: procedure ICS( $A, \mathbf{p}, k, c, l, \tau$ )
2:    $S \leftarrow \{1, 2, \dots, n\}$ 
3:    $C, \tilde{V}, \tilde{\Sigma}, S \leftarrow \text{SAMPLE COLUMNS}(A, S, \mathbf{p}, c); t \leftarrow \min(l, \max(r : \tilde{\sigma}_r \neq 0))$ 
4:    $\tilde{\mathbf{u}}_i \leftarrow C\tilde{\mathbf{v}}_i/\tilde{\sigma}_i$ 
5:    $s \leftarrow \text{card}(S)$ 
6:    $\xi_i \leftarrow 0$  where  $i = 1, 2, \dots, k$ 
7:   while  $\exists \xi_i : \xi_i < \tau$  and  $s > 0$  do
8:      $p_i \leftarrow 1/s$ ; or  $p_i \leftarrow \|\mathbf{a}_i - \tilde{U}\tilde{U}^T\mathbf{a}_i\|^2 / \sum \|\mathbf{a}_i - \tilde{U}\tilde{U}^T\mathbf{a}_i\|_F^2$ , where  $i \in S$ 
9:      $C, \hat{V}, \hat{\Sigma}, S \leftarrow \text{SAMPLE COLUMNS}(A, S, \mathbf{p}, c); t \leftarrow \min(l, \max(r : \hat{\sigma}_r \neq 0))$ 
10:     $\hat{\mathbf{u}}_i \leftarrow C\hat{\mathbf{v}}_i/\hat{\sigma}_i$  where  $i = 1, 2, \dots, t$ 
11:     $s \leftarrow \text{card}(S)$ 
12:     $\tilde{U}, \hat{\Sigma} \leftarrow \text{BLOCK MERGE}(\tilde{U}, \tilde{\Sigma}, \hat{U}, \hat{\Sigma}, l)$ 
13:     $\xi_i \leftarrow \tilde{\mathbf{u}}_i^T \hat{\mathbf{u}}_i$  where  $i = 1, 2, \dots, k$ 
14:     $\tilde{U} \leftarrow \hat{U}; \tilde{\Sigma} \leftarrow \hat{\Sigma}$ 
15:  end while
16:  return  $\tilde{\mathbf{u}}_i, \tilde{\sigma}_i$  where  $i = 1, 2, \dots, k$ 
17: end procedure
18: procedure SAMPLE COLUMNS( $A, S, \mathbf{p}, c$ )
19:    $\mathbf{I}_s \leftarrow \{s_i : \Pr[s_i = \alpha] = p_\alpha \in \mathbf{p}, s_i \in S\}$ 
20:    $\mathbf{I}_d \leftarrow s_i : \forall \text{ distinct } s_i \in \mathbf{I}_s; g \leftarrow \text{card}(\mathbf{I}_d)$ 
21:    $S \leftarrow S \setminus \mathbf{I}_d$ 
22:    $\mathbf{c}_i \leftarrow \mathbf{a}_{d_i}$ , where  $d_i \in \mathbf{I}_d$  and  $i = 1, 2, \dots, g$ 
23:    $\tilde{V}\tilde{\Sigma}^2\tilde{V} \leftarrow \text{SVD}(C^T C)$ 
24:   return  $C, \tilde{V}, \tilde{\Sigma}, S$ 
25: end procedure

```

Algorithm 5 details the steps involved. The tolerance parameter, τ , is a measure of the upper bound for the angle between modes computed in successive iterations or the principal angles of the subspaces computed in successive iterations. The main difference between our iteration and the adaptive sampling algorithm is that, in each iteration we have an updated approximation of the POD modes and the dominant subspace. The penalty is finding the SVD of the sampled columns. This can be mitigated if we use the procedure SAMPLE AND SCALE UNIQUE ROWS in Algorithm 3 and use the SVD of W to get the approximate POD modes and singular values in each iteration. Note that, this way the modes obtained may not be orthonormal. To rectify this, we orthonormalize the modes. This is done only in the first approximation of the modes since in the subsequent iterations, orthonormalization is implicit in the MAT algorithm. Algorithm 6 contains the steps.

Since we do not scale columns, the error in the singular values could be significant if the total number of columns sampled is much less than the number of columns in the matrix. If this is the case, one can use the technique followed in the adaptive sampling method i.e. after the modes have converged, the singular values can be obtained by computing the SVD of $\tilde{U}_k^T A$. Note that we will have only k basis vectors, so that this matrix is small.

Algorithm 6 Iterative SVD algorithm with column and row sampling; Inputs: same as Algorithm 5 and additionally w , number of rows to sample.

```

1: procedure ICRS( $A, \mathbf{p}, k, c, w, l, \tau$ )
2:    $S \leftarrow \{1, 2, \dots, n\}$ 
3:    $C, \tilde{V}, \tilde{\Sigma}, S \leftarrow \text{SAMPLE COLUMNS AND ROWS}(A, S, \mathbf{p}, c, w)$ 
4:    $t \leftarrow \min(l, \max(r : \tilde{\sigma}_r \neq 0))$ ;  $\mathbf{u}_i \leftarrow C\tilde{\mathbf{v}}_i, i \in \{1, 2, \dots, l\}$ 
5:    $Q, R \leftarrow \text{QR}(U); U, \tilde{\Sigma}, V \leftarrow \text{SVD}(R); \tilde{U} \leftarrow QU$  ▷ for orthonormal  $\tilde{U}$ 
6:    $s \leftarrow \text{card}(S)$ 
7:    $\xi_i \leftarrow 0$  where  $i = 1, 2, \dots, k$ 
8:   while  $\exists \xi_i : \xi_i < \tau$  and  $s > 0$  do
9:      $p_i \leftarrow 1/s$ ; or  $p_i \leftarrow \|\mathbf{a}_i - \tilde{U}\tilde{U}^T \mathbf{a}_i\|^2 / \sum \|\mathbf{a}_i - \tilde{U}\tilde{U}^T \mathbf{a}_i\|_F^2$ , where  $i \in S$ 
10:     $C, \hat{V}, \hat{\Sigma}, S \leftarrow \text{SAMPLE COLUMNS AND ROWS}(A, S, \mathbf{p}, c, w); t \leftarrow \min(l, \max(r : \hat{\sigma}_r \neq 0))$ 
11:     $\hat{\mathbf{u}}_i \leftarrow C\hat{\mathbf{v}}_i / \hat{\sigma}_i$  where  $i = 1, 2, \dots, t$ 
12:     $s \leftarrow \text{card}(S)$ 
13:     $\hat{U}, \hat{\Sigma} \leftarrow \text{BLOCK MERGE}(\tilde{U}, \tilde{\Sigma}, \hat{U}, \hat{\Sigma}, l)$ 
14:     $\xi_i \leftarrow \hat{\mathbf{u}}_i^T \hat{\mathbf{u}}_i$  where  $i = 1, 2, \dots, k$ 
15:     $\tilde{U} \leftarrow \hat{U}; \tilde{\Sigma} \leftarrow \hat{\Sigma}$ 
16:  end while
17:  return  $\tilde{\mathbf{u}}_i, \tilde{\sigma}_i$  where  $i = 1, 2, \dots, k$ 
18: end procedure
19: procedure SAMPLE COLUMNS AND ROWS( $A, S, \mathbf{p}, c, w$ )
20:    $\mathbf{I}_s \leftarrow s_i : \Pr[s_i = \alpha] = p_\alpha \in \mathbf{p}, s_i \in S$ 
21:    $\mathbf{I}_d \leftarrow s_i : \forall \text{ distinct } s_i \in \mathbf{I}_s; g \leftarrow \text{card}(\mathbf{I}_d)$ 
22:    $S \leftarrow S \setminus \mathbf{I}_d$ 
23:    $\mathbf{c}_i \leftarrow \mathbf{a}_{d_i}$ , where  $d_i \in \mathbf{I}_d$  and  $i = 1, 2, \dots, g$ 
24:    $W \leftarrow \text{SAMPLE AND SCALE UNIQUE ROWS}(C, w)$  ▷ see Algorithm 3
25:    $\tilde{V}\tilde{\Sigma}^2\tilde{V} \leftarrow \text{SVD}(W^T W)$ 
26:   return  $C, \tilde{V}, \tilde{\Sigma}, S$ 
27: end procedure

```

Table 4: Average time taken (in seconds) by $\text{SVD}(A)$ and $\text{SVD}(A^T A)$ for different datasets. Note that SVD of Yale faces could not be computed in our test system since it does not fit in the system’s memory.

Dataset	SVD(A)		SVD($A^T A$)	
	single thread	4 threads	single thread	4 threads
V_{2D}	25.28	13.94	8.39	2.75
Faces	0.35	0.17	0.13	0.069
Cropped Yale faces	34.04	16.43	15.23	6.86
Yale faces	-	-	-	-

5 Results

All algorithms are run in a 4 core Intel® Core™ i7-6700K processor that runs at a maximum clock frequency of 4GHz with hyper-threading on. The system has a 32GB RAM. The algorithms are written in Python and run in Python version 3.5.3. It uses *numpy* version 1.12.1-3, *scipy* version 0.18.1-2 and *openBLAS* version 0.2.19-3, which is multi-threaded. Double precision was used for all computations. The random number generator in *numpy* is used. Runtimes and speedup values are an average of five runs. We report speed-up obtained when *openBLAS* is run using a single thread, to give a measure of the operation count in each algorithm and four threads (since our system is a four core system), which gives an indication of how the runtime scales with number of threads. We have not explicitly parallelised our algorithm and any improvement with multiple threads is entirely due to *openBLAS*.

If A is a tall and skinny matrix, computing $\text{SVD}(A)$ using $\text{SVD}(A^T A)$ is faster. This is because $\text{SVD}(A)$ takes approximately βmn^2 floating point operations (FLOPs). $\text{SVD}(A^T A)$ requires mn^2 FLOPs to compute $A^T A$, $(\beta + 16)n^3$ to compute $\text{SVD}(A^T A)$ and another mn^2 operations to compute u_i from Av_i/σ_i . Assuming $\beta = 6$ [31, 32], this gives $m/(m/3 + (1 + 8/3)n)$ speedup. For example, in V_{2D} with $m = 132098$ and $n = 1024$, the expected speed up is 2.76 which is close to what we get, as seen in Table 4. Since the LTSVD and CTSVD algorithms compute SVD using $X^T X$, we benchmark the speedup of the algorithms with respect to $\text{SVD}(A^T A)$.

Fig. 6 demonstrates the runtime efficiency of the LTSVD_US and CTSVD_US algorithms with respect to (a) $\text{SVD}(A^T A)$ and (b) LTSVD and CTSVD. The speedup with respect to $\text{SVD}(A^T A)$ is of the order of $\approx n^2/g^2$ and it is seen that very large speedups are obtained, especially for the case C3. We obtain a minimum of $3\times$ speedup with a single thread and $2\times$ with 4 threads. The speedup obtained with respect to LTSVD and CTSVD is mainly dependent on the number of distinct columns sampled compared to the actual number of columns sampled. The speedup will be $\approx c^2/g^2$. As seen in Fig. 6, for cases C1 and C2 LTSVD_US and CTSVD_US have a $1.2\text{--}3.5\times$ speedup over LTSVD and CTSVD, as expected. For C3, the runtime is the almost the same, indicating that there is not much penalty in searching for distinct indices when the number of sampled columns is small.

The mean-centered data matrix for Yale faces dataset requires 40GB memory and does not fit in the RAM. There are two possible ways to compute the POD modes of this dataset: (a) run LTSVD/CTSVD on this data by reading the data in chunks that fit in the memory and deleting it after each use or (b) do an incremental computation by running LTSVD_US/CTSVD_US on each block of the partitioned data and then merging the SVD of these blocks using the MAT algorithm. In order to run LTSVD/CTSVD on the full matrix, it needs to be fetched twice for LTSVD and thrice for CTSVD including computation

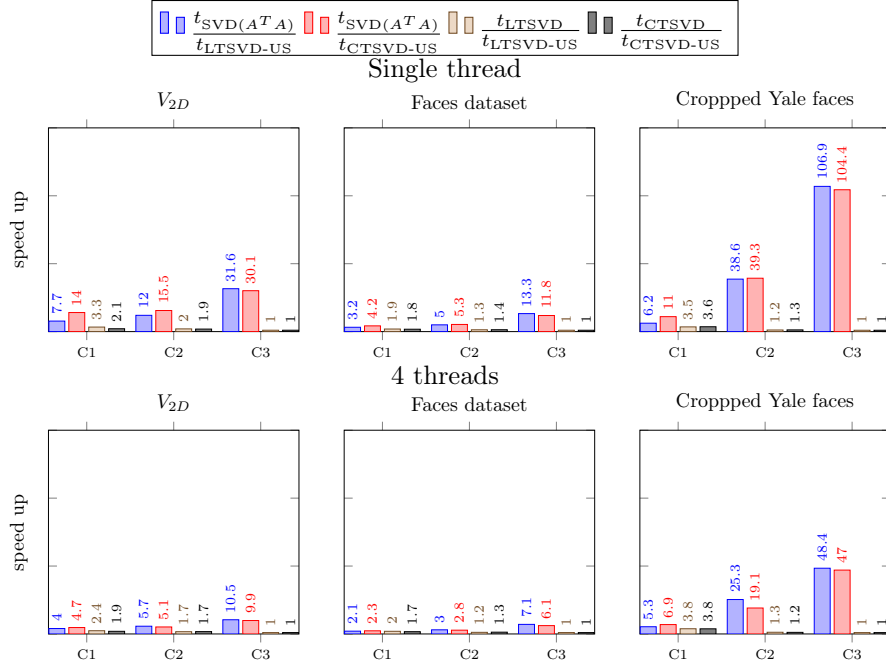


Figure 6: Speed up obtained due to using unique sampling algorithms with respect to LTSVD, CTSVD and $SVD(A^T A)$ when run on different datasets for different parameter values, as given in Table 2.

of sampling probabilities. Also, the number of sampled columns has to be small enough to fit in RAM for the SVD computation. This process is severely bottlenecked by disk access times. We did an incremental computation after partitioning the matrix into t blocks. We first computed the number of columns c to be sampled from the full matrix, for a given set of error parameters. $c_t = \frac{c}{t}$ columns (columns and rows in the case of incremental CTSVD_US) are sampled in each partition. Note that the number of rows sampled in each partition for CTSVD_US is smaller than when CTSVD_US is run on the full matrix. Consequently, use of CTSVD_US for each partition followed by MAT, tends to have a lower accuracy than running CTSVD_US on the full matrix in many cases.

For the YF dataset, we partitioned the matrix into four blocks. Table 5 shows the parameter values for which the incremental algorithms were run. The parameters were chosen to satisfy the following.

1. Sample close to the same total number of columns as in the case of C1 of Yale faces (B1 in Table 5). $c_t = w_t = \frac{c}{4}$.
2. Increase the value of c so that the number of rows in each partition increases. The aim is to get similar accuracy as CTSVD_US, C1. This is B2 in Table 5.

Fig. 7 shows that in the case of LTSVD B1, for $k > 15$, the mode angle accuracy is better than that of LTSVD C1 even though the probability distribution with respect to the full matrix is sub-optimal. On partitioning the matrix, we possibly get a better selection of columns corresponding to the smaller singular values. As expected, in the case of CTSVD B1, the mode angles are substantially larger than CTSVD C1. It can be rectified

by oversampling from the blocks. B2 in Fig. 7 demonstrates how oversampling improves the accuracy in the modes. However, since the results depend on the sampling probability distributions based on row norms, it is not clear how much oversampling is required in general.

Table 5: Number of columns and/or rows sampled by incremental LTSVD and incremental CTSVD when run on Yale faces. t is the number of blocks and c_t and w_t are the number of columns and rows sampled from each block.

Case	t	k	LTSVD		CTSVD	
			c	c_t	c	$c_t = w_t$
B1	4	20	9924	2481	10488	2622
B2	4	20	12252	3063	12920	3230

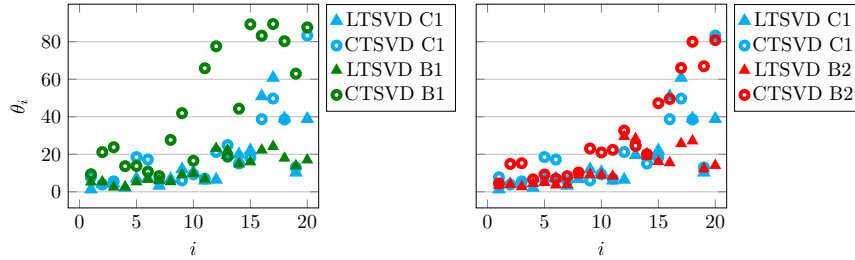


Figure 7: First k mode angles, θ_i , of Yale faces computed by the incremental sampling algorithms for different number of sampled columns/rows, as given in Table 5.

We tested the performance of the iterative algorithms with two different convergence criteria: angles between the modes obtained in successive iterations and the principal angles between the subspaces computed in successive iterations. As indicated previously, we tried two different sampling strategies - S1 based on a uniform distribution and S2 based on row/column norms of the orthogonal components. Using ϵ and δ around 0.6 – 0.7 resulted in a reasonable tradeoff between the number of columns (and rows) sampled in each iteration and the number of iterations. For the Faces dataset, we chose a higher ϵ, δ since the number of columns in the matrix is quite small. Only S1 was used in the iterative algorithms for YF, since the overhead for computing the orthogonal complement in each iteration proved to be large.¹ Table 6 lists the parameter values used for the iterative algorithms.

Table 6: Parameter values (k, ϵ, δ) used in ICS and ICRS algorithms for various datasets

Case	V_{2D} , CYF	Faces	YF
	k, ϵ, δ	k, ϵ, δ	k, ϵ, δ
ICS&ICRS			
I1	2, 0.7, 0.6	2, 0.7, 0.6	5, 0.6, 0.6
I2	10, 0.7, 0.6	10, 1, 0.75	20, 0.6, 0.6

¹ For YF, the runs for the iterative algorithm were made in a different system, a 20 core Intel® Xeon® CPU E5-2630V4 processor that runs at a maximum clock frequency of 2.2GHz with hyper-threading on, with 64GB of RAM.

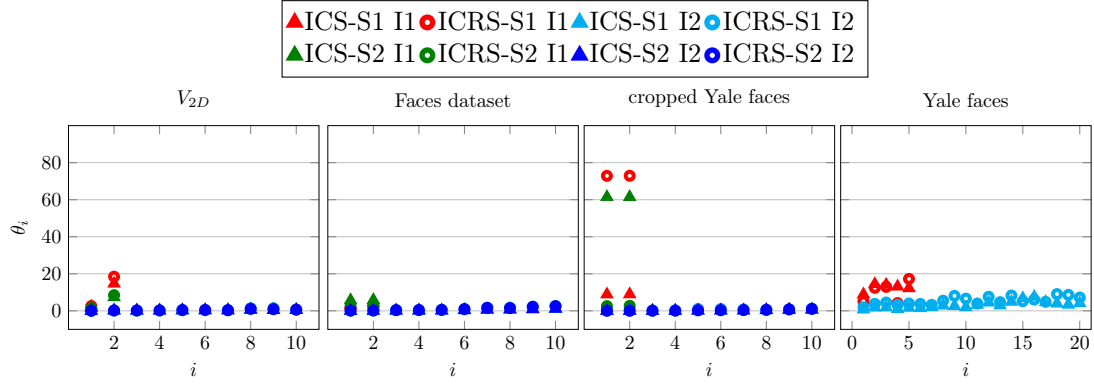


Figure 8: First k mode angles, θ_i , of different datasets computed by iterative algorithms with convergence of mode angles used as the stopping criterion.

Fig. 8 shows the first k mode angles computed by the iterative algorithms using either S1 or S2 from the second iteration. In these computations, tolerance on the cosine similarity between POD modes computed in successive iterations, τ , is set to 0.99. It is seen that except for the first two modes in CYF, all the POD modes are approximated very well. For $k = 10$ (I2), both S1 and S2 give very similar results, but for $k = 2$ (I1), there is no clear better performer. In the case of YF, ϵ, δ set for the iterative algorithms is much larger than those in LTSVD and CTSVD algorithms (see Table 2). Even so, for I2 ($k = 20$) accuracy of the POD modes is much better than in LTSVD and CTSVD. But the accuracy is slightly worse for I1 ($k = 5$) when compared to LTSVD and CTSVD.

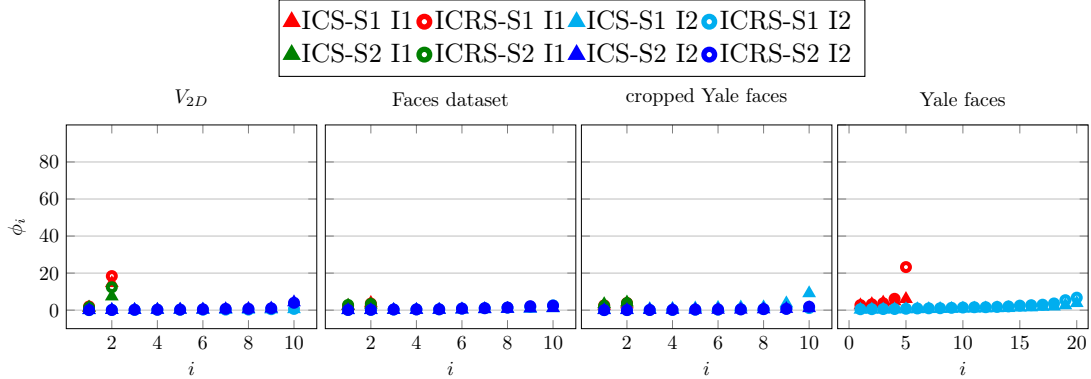


Figure 9: First k principal angles, ϕ_i , of different datasets computed by the iterative algorithms. The iteration is based on convergence of principal angles.

We also ran the algorithm with convergence of the principal angles as the criterion with the same value for τ . Fig. 9 shows the principal angles between the subspaces spanned by the approximate modes and the modes obtained using the truncated SVD. The algorithms give similar results as in Fig. 8 for faces and V_{2D} datasets. As expected, for the CYF dataset, the subspace spanned by the first two modes is better approximated than the individual modes.

Fig. 10 and Fig. 11 contain the speedup obtained when the iterative algorithms are run

with mode angle and principal angles used as the convergence criterion respectively. For both cases, $\tau = 0.99$. The figures contain (a) speedup with respect to $\text{SVD}(A^T A)$ and (b) speedup on sampling using a uniform distribution (S1) with respect to S2. It is seen from the figures that except for one case, significant speedup is obtained for all datasets both for single and multithreaded execution. As expected, in comparison to S2, S1 is faster (at least 20% faster to at most 9 times faster). We found that for $k = 10$ (I2), nearly all columns were sampled for the Faces, V_{2D} and CYF datasets when convergence was achieved, both in terms of mode and principal angles. For I1 ($k = 2$), the number of columns sampled was substantially lower than n in all cases. It is interesting that the speedup is large, even when all the columns are sampled. For the V_{2D} and Faces datasets, the speedup is almost the same for both convergence criteria. However, for CYF, speed up obtained is substantially larger when principal angles are used for $k = 2$. This is because a significantly lower number of columns is sampled. In datasets containing faces, τ of 0.95 seemed sufficient. This will further improve the runtime efficiency.

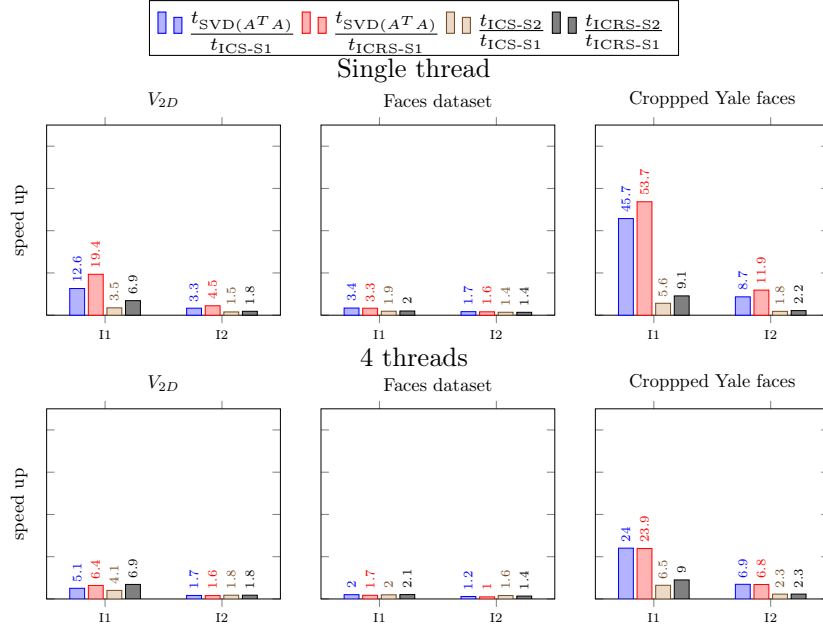


Figure 10: Speed up obtained due to using iterative algorithms with respect to $\text{SVD}(A^T A)$ with convergence of mode angles as the stopping criterion.

Fig. 12 shows few POD modes of V_{2D} computed by the iterative algorithms. It can be seen that the POD modes of V_{2D} are approximated well, with not much visually apparent distortions.

6 Conclusion

In this paper, we modified the LTSVD and CTSVD algorithms proposed in [1] and established an equivalence between the modified and original algorithms with respect to the left-singular vectors and singular values. We derived a relationship between the right-singular vectors obtained in the two cases. The algorithms were run on four datasets of various sizes.

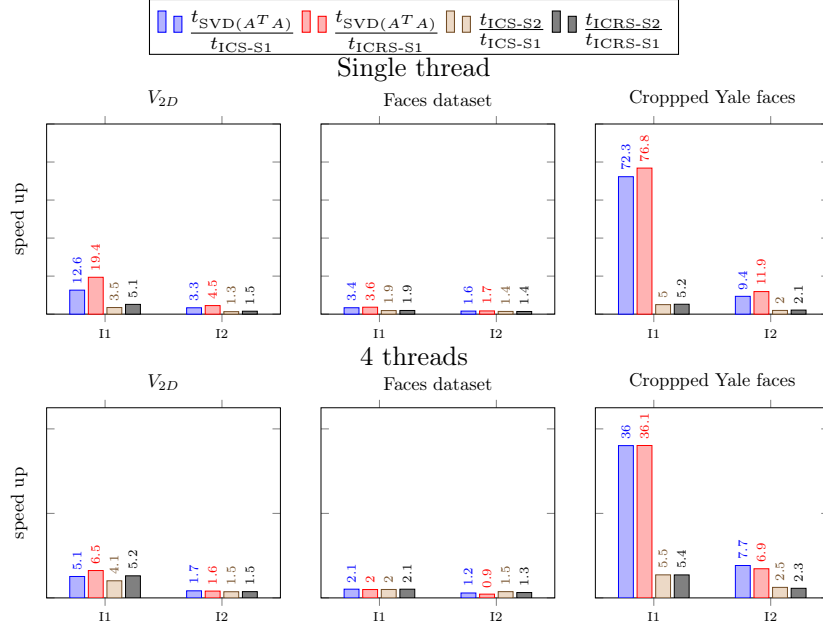


Figure 11: Speed up obtained due to using iterative algorithms with respect to $\text{SVD}(A^T A)$ with convergence of principal angles as the stopping criterion.

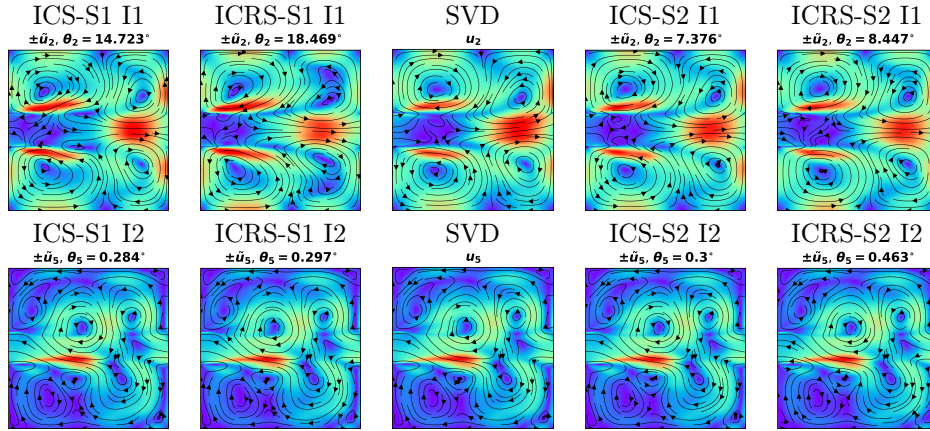


Figure 12: Second and fifth POD modes of V_{2D} computed by SVD and the iterative algorithms.

The results show the modifications led to a significant speedup for low and moderate values of the error parameters. The modifications are independent of the sampling probabilities.

We also used a previously proposed MAT algorithm to implement an incremental sampling-based algorithm for large datasets that do not fit in the RAM. The incremental algorithm gave comparable or better results when LTSVD_US was used for each partition, but slightly worse when CTSVD_US was used. This is due to the much smaller number of rows sampled in each partition. A slight oversampling of rows and columns, resulted in similar errors. An improvement to our algorithm would be to just oversample rows. However, the results are empirical and it would be useful to have error bounds to predict the amount of oversampling required.

We proposed an iterative algorithm to improve the modes/subspaces spanned by the modes. Unlike the earlier methods used for multiple rounds of sampling, we estimate the POD modes in each iteration and stop sampling when no further improvement is obtained in either the modes or subspaces spanned by the modes. The algorithm resulted in good accuracies with significant improvement in runtime even if all columns are sampled when convergence is achieved. We found that using column-norm sampling in the first round and uniform sampling in subsequent rounds resulted in good speedups, with accuracy comparable to using norm of the orthogonal component of the columns. An extension would be to use a combination of incremental and iterative algorithms to get better accuracies and speedup for large matrices.

References

- [1] Petros Drineas, Ravi Kannan, and Michael W. Mahoney. Fast monte carlo algorithms for matrices ii: Computing a low-rank approximation to a matrix. *SIAM Journal on Computing*, 36(1):158–183, 2006.
- [2] Kunihiko Taira, Steven L Brunton, Scott TM Dawson, Clarence W Rowley, Tim Colonius, Beverley J McKeon, Oliver T Schmidt, Stanislav Gordeyev, Vassilios Theofilis, and Lawrence S Ukeiley. Modal analysis of fluid flows: An overview. *AIAA Journal*, pages 4013–4041, 2017.
- [3] N. Muller, L. Magaia, and B. Herbst. Singular value decomposition, eigenfaces, and 3d reconstructions. *SIAM Review*, 46(3):518–545, 2004.
- [4] M. A. Turk and A. P. Pentland. Face recognition using eigenfaces. In *Proceedings. 1991 IEEE Computer Society Conference on Computer Vision and Pattern Recognition*, pages 586–591, June 1991.
- [5] Orly Alter, Patrick O. Brown, and David Botstein. Singular value decomposition for genome-wide expression data processing and modeling. *Proceedings of the National Academy of Sciences*, 97(18):10101–10106, 2000.
- [6] Markus Ringnér. What is principal component analysis? *Nature Biotechnology*, 26:303–304, 2008.
- [7] N. Halko, P. G. Martinsson, and J. A. Tropp. Finding structure with randomness: probabilistic algorithms for constructing approximate matrix decompositions. *SIAM Review*, 53(2):217–288, 2011.

- [8] T. Sarlos. Improved approximation algorithms for large matrices via random projections. In *2006 47th Annual IEEE Symposium on Foundations of Computer Science (FOCS'06)*, pages 143–152, Oct 2006.
- [9] V. Rokhlin, A. Szlam, and M. Tygert. A randomized algorithm for principal component analysis. *SIAM Journal on Matrix Analysis and Applications*, 31(3):1100–1124, 2010.
- [10] N Benjamin Erichson, Sergey Voronin, Steven L Brunton, and J Nathan Kutz. Randomized matrix decompositions using `r`, 2016. arXiv:1608.02148.
- [11] Dimitris Achlioptas and Frank Mcsherry. Fast computation of low-rank matrix approximations. *J. ACM*, 54(2), April 2007.
- [12] Petros Drineas, Eleni Drinea, and Patrick S. Huggins. An experimental evaluation of a monte-carlo algorithm for singular value decomposition. In Yannis Manolopoulos, Skevos Evripidou, and Antonis C. Kakas, editors, *Advances in Informatics*, pages 279–296, Berlin, Heidelberg, 2003. Springer Berlin Heidelberg.
- [13] P. Drineas, A. Frieze, R. Kannan, S. Vempala, and V. Vinay. Clustering large graphs via the singular value decomposition. *Mach. Learn.*, 56(1-3):9–33, June 2004.
- [14] Alan Frieze, Ravi Kannan, and Santosh Vempala. Fast monte-carlo algorithms for finding low-rank approximations. *J. ACM*, 51(6):1025–1041, November 2004.
- [15] Petros Drineas, Michael W. Mahoney, and S. Muthukrishnan. Relative-error *cur* matrix decompositions. *SIAM J. Matrix Anal. Appl.*, 30(2):844–881, September 2008.
- [16] Amit Deshpande, Luis Rademacher, Santosh Vempala, and Grant Wang. Matrix approximation and projective clustering via volume sampling. In *Proceedings of the seventeenth annual ACM-SIAM symposium on Discrete algorithm*, pages 1117–1126. Society for Industrial and Applied Mathematics, 2006.
- [17] A. Deshpande and S. Vempala. Adaptive sampling and fast low-rank matrix approximation. In *Proceedings of the 9th International Conference on Approximation Algorithms for Combinatorial Optimization Problems, and 10th International Conference on Randomization and Computation*, APPROX’06/RANDOM’06, pages 292–303, Berlin, Heidelberg, 2006. Springer-Verlag.
- [18] Petros Drineas and Michael W. Mahoney. Randnla: Randomized numerical linear algebra. *Commun. ACM*, 59(6):80–90, May 2016.
- [19] Michael B. Cohen, Cameron Musco, and Christopher Musco. Input sparsity time low-rank approximation via ridge leverage score sampling, 2015. arXiv:1511.07263.
- [20] Mu Li, Gary L. Miller, and Richard Peng. Iterative row sampling. In *Proceedings of the 2013 IEEE 54th Annual Symposium on Foundations of Computer Science*, FOCS ’13, pages 127–136, Washington, DC, USA, 2013. IEEE Computer Society.
- [21] Michael B. Cohen, Yin Tat Lee, Cameron Musco, Christopher Musco, Richard Peng, and Aaron Sidford. Uniform sampling for matrix approximation. In *Proceedings of the 2015 Conference on Innovations in Theoretical Computer Science*, ITCS ’15, pages 181–190, New York, NY, USA, 2015. ACM.

- [22] I. Yamazaki, S. Tomov, and J. Dongarra. Sampling algorithms to update truncated svd. In *2017 IEEE International Conference on Big Data (Big Data)*, pages 817–826, Dec 2017.
- [23] Aditya Krishna Menon and Charles Elkan. Fast algorithms for approximating the singular value decomposition. *ACM Trans. Knowl. Discov. Data*, 5(2):13:1–13:36, February 2011.
- [24] Nam H. Nguyen, Thong T. Do, and Trac D. Tran. A fast and efficient algorithm for low-rank approximation of a matrix. In *Proceedings of the Forty-first Annual ACM Symposium on Theory of Computing*, STOC '09, pages 215–224, New York, NY, USA, 2009. ACM.
- [25] Vinita Vasudevan and M. Ramakrishna. A hierarchical singular value decomposition algorithm for low rank matrices, October 2017. arXiv:1710.02812.
- [26] AT&T Laboratories Cambridge. The database of faces, 2002.
- [27] K.C. Lee, J. Ho, and D. Kriegman. Acquiring linear subspaces for face recognition under variable lighting. *IEEE Trans. Pattern Anal. Mach. Intelligence*, 27(5):684–698, 2005.
- [28] A.S. Georghiades, P.N. Belhumeur, and D.J. Kriegman. From few to many: Illumination cone models for face recognition under variable lighting and pose. *IEEE Trans. Pattern Anal. Mach. Intelligence*, 23(6):643–660, 2001.
- [29] Åke Björck and Gene H. Golub. Numerical methods for computing angles between linear subspaces. *Mathematics of Computation*, 27(123):579–594, 1973.
- [30] M. A. Iwen and B. W. Ong. A distributed and incremental svd algorithm for agglomerative data analysis on large networks. *SIAM J. Matrix Analysis Applications*, 37:1699–1718, 2016.
- [31] Gene H Golub and Charles F Van Loan. *Matrix computations*. Hindustan Book agency, 3 edition, 2007.
- [32] Åke Björck. *Numerical methods in matrix computations*, volume 59. Springer, 2015.